Malaysian Journal of Analytical Sciences



EQUIVALENT CIRCUIT ANALYSIS OF LaZrTa₃O₁₁ CERAMIC SYNTHESISED BY USING THE CONVENTIONAL SOLID-STATE METHOD

(Analisis Litar Sepadan Seramik LaZrTa₃O₁₁ Disintesis dengan Menggunakan Kaedah Keadaan Pepejal Konvensional)

Fadhlina Che Ros* and Jumiah Hassan

Physics Department, Centre for Defence Foundation Studies, Universiti Pertahanan Nasional Malaysia, Kem Sungai Besi 57000, Kuala Lumpur, Malaysia

*Corresponding author: fadhlina@upnm.edu.my

Received: 13 November 2019; Accepted: 3 September 2020; Published: 12 October 2020

Abstract

LaZrTa₃O₁₁ ceramic with α-U₃O₈-type structure has been prepared by using the conventional solid state-route and studied by using powder X-ray diffraction for phase analysis and impedance spectroscopy for electrical measurements. It has hexagonal unit cell with space group P6₃22 at room temperature. LaZrTa₃O₁₁ is reported to be isostructural with CaTa₄O₁₁ and Ag₂Nb₄O₁₁; the structure is related to U₃O₈-structure, where it consists of single layers of edge-sharing pentagonal Ta-O bipyramids alternating with layers of edge-sharing octahedra. The impedance spectroscopy response showed that LaZrTa₃O₁₁ exhibited a typical insulating behaviour at room temperature, with permittivity, $\varepsilon \sim 19$. It was a highly resistive material with $R >> 10^9 \Omega$ at temperature below 500° C and as the temperature increased, frequency-dependence of alternating current conductivities at high frequency was clearly visible. The electrical properties of LaZrTa₃O₁₁ is best modelled by using non-Debye response circuit that consists of a parallel combination of a resistor, capacitor, and a constant phase element.

Keywords: LaZrTa₃O₁₁, dielectrics, high-temperature ceramics, lanthanide-oxide, non-Debye circuit

Abstrak

Seramik LaZrTa₃O₁₁ dengan struktur jenis α-U₃O₈ telah disediakan melalui kaedah keadaan pepejal konvensional dan dikaji dengan menggunakan pembelauan sinar-X untuk analisis fasa dan spektroskopi impedans untuk kajian sifat keelektrikan. Ia mempunyai sel unit heksagonal dengan kumpulan ruang P6322 pada suhu bilik. LaZrTa3O11 dilaporkan mempunyai sama struktur dengan CaTa₄O₁₁ dan Ag₂Nb₄O₁₁; struktur tersebut adalah berkait dengan struktur U₃O₈ di mana ia terdiri daripada satu lapisan pentagonal bypiramid Ta-O berkongsi-sisi, berselang-seli dengan lapisan-lapisan oktahedra yang berkongsi-sisi. Tindak-balas spektroskopi impedans menunjukkan bahawa seramik LaZrTa₃O₁₁ mempamerkan sifat penebat yang tipikal pada suhu bilik, dengan kebolehtelapan, $\varepsilon \sim 19$. Ia adalah bahan berkerintangan tinggi dengan R >> $10^9 \Omega$ pada suhu di bawah 500° C dan apabila suhu meningkat, kebergantungan frekuensi konduktiviti arus ulang alik pada frekuensi tinggi jelas kelihatan. Model terbaik sifat keelektrikan bagi seramik LaZrTa₃O₁₁ adalah menggunakan litar non-Debye yang terdiri daripada kombinasi selari perintang, kapasitor dan elemen fasa pemalar.

Kata kunci: LaZrTa₃O₁₁, dielektrik, seramik bersuhu tinggi, oksida lanthanid, litar non-Debye

Introduction

Lanthanum zirconium tritantalum hendecaoxide (LaZrTa₃O₁₁) exhibits layers of edge-sharing pentagonal (Ta, Zr)-O₇ bipyramids that alternate with layers of edge-sharing LaO₈ polyhedra and (Ta,Zr)-O₆ octahedra. Many researchers have reported on its structure, namely Zheng and West reported LaZrTa₃O₁₁ ceramic as orthorhombic, a face-centred cell that belongs to one of the three possible space groups, Fmmm, Fmm2, or F222, a = 10.890(3), b = 12.450(3), and c = 6.282(2) Å, butlater in 1992, Grins and Nygren reported the true symmetry of LaZrTa₃O₁₁ as the hexagonal space group $P6_322$, a = 62824(2), c = 12.4469(7) Å. Literature have also reported that LaZrTa₃O₁₁ is isostructural with CaTa₄O₁₁ and the newly-discovered ferroelectric material silver niobate, Ag₂Nb₄O₁₁ [1,2]. The nature of LaZrTa₃O₁₁ is shown in Figure 1.

The unique structure of LaZrTa₃O₁₁ has attracted much interest among researchers except for its electrical properties of which even at the highest temperature, LaZrTa₃O₁₁ is very poor in electrical conductivity due to its extremely large amount of resistance [3-6]. No detailed studies on its electrical properties have been published so far. Recently, the researchers have reported eight new phases of similar structure to LaZrTa₃O₁₁ with the general formula REMY₃O₁₁, namely LaHfTa, LaHfNb, LaZrNb, PrHfTa, NdHfTa, NdHfNb, SmHfTa, and GdHfTa, where all phases had highly insulated permittivities in the range of 17 to 50 [4]. Insulators like LaZrTa₃O₁₁ have possible applications as substrate or plastic-based laminates due to their low conductivity even at a high temperature. Laminates are dominant in a relatively low technology application, such as casings for radios and televisions, whereas substrates are extensively used for demanding application in communications, military, space technologies, and automotive control [7]. In this study, the electrical properties and equivalent circuit analysis of LaZrTa₃O₁₁ at different temperatures were reported by using impedance spectroscopy (IS) method as a function of frequency. The analysis and modelling of IS data provided useful information about physical processes

that occurred within the samples, which can be represented by a capacitor, C, resistor, R, and constant phase element (CPE) components of the proposed equivalent circuit.

Materials and Methods

LaZrTa₃O₁₁ was synthesized by using conventional solid-state routes, namely La₂O₃, Ta₂O₅ and ZrO₂ (99.9% pure Stanford Materials), which were dried overnight and stored under vacuum prior to being used. Mixtures totaling 5 g were weighed, mixed, and ground with acetone by using an agate mortar and pestle and were subsequently dried, pressed into pellets, and fired in a platinum (Pt) crucible in an electric muffle furnace at 1500 °C for 12 hours with plenty of air. The sample was removed from the furnace, crushed into a fine powder, repelleted, and returned to the furnace for another 12 h reaction at 1500° C intermittently for up to 3 days to obtain a single-phase product.

STOE STADI P diffractometer, Cu $K\alpha_1$ radiation (λ = 1.54056 Å) was used in X-ray diffraction (XRD). External silicon standard, NIST 640d Si was used for line position calibration in which data were managed and compared against reference data in the ICDD's PDF-2 database by using STOE WinX^{POW} software package. Data were collected for \sim 4 hours and corrected for absorption.

For electrical measurement, Pt paste electrodes were fabricated on the opposite pellet faces of cylindrical sintered pellets and hardened by gradually heating in the air at 800 °C for 2 hours. The samples with electrodes attached were placed into a conductivity jig and heated in a small tube furnace within the temperature range of room temperature to 800 °C. Electrical data were recorded by using a Hewlett Packard 4192A Impedance Analyser over the frequency range of 10 Hz to 1 MHz, with an alternating current (AC) voltage of 100 mV. The impedance raw data were corrected for the overall geometric factor of ceramic and data analysis was performed by using the software program, ZView.

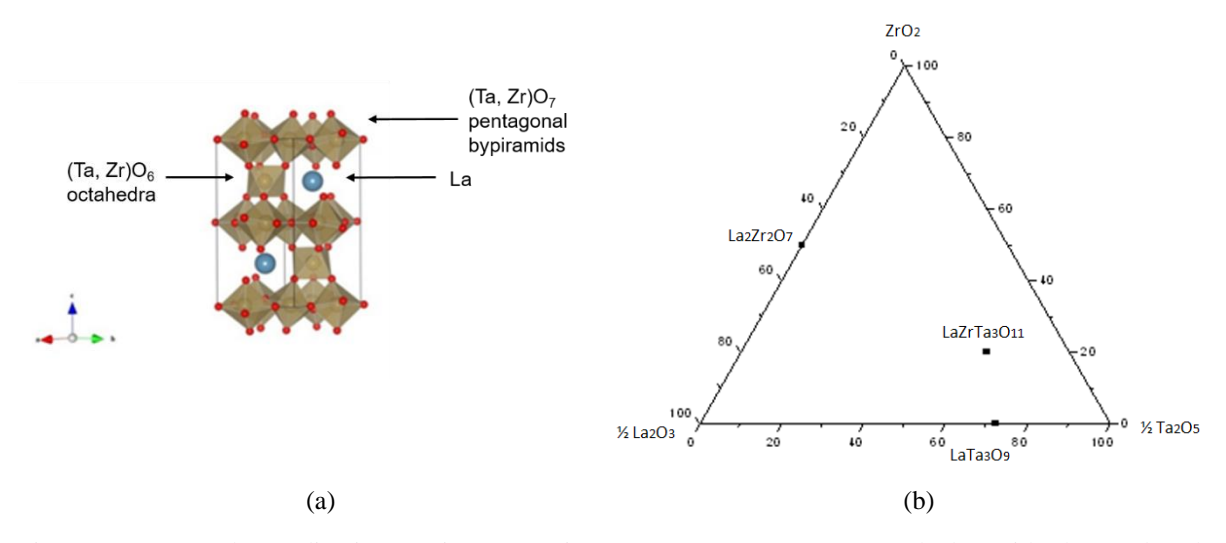


Figure 1. (a) Local coordination environments in LaZrTa $_3O_{11}$; two TaO $_6$ octahedra with three edge-sharing pentagonal bipyramids above and below near La positions, (b) LaZrTa $_3O_{11}$ within the ternary diagram ½ La $_2O_3$ - ½ Ta $_2O_5$ – ZrO $_2$

Results and Discussion

Phase analysis

intensities relative peak of LaZrTa₃O₁₁ corresponded well with the calculated pattern reported in the ICDD - PDF card 81, 1935. The XRD data were indexed on the hexagonal space group, P6322 and the data were collected over a 2θ -range from 10° to 70° . The sample was not in a single-phase due to the existence of impurities even at 72 hours of firing. The lattice parameters of the obtained LaZrTa₃O₁₁ were slightly bigger: a = 6.28724(4), c = 12.4525(1) Å as compared to the literature [2]: a = 6.2824, c = 12.4469 Å, which may be due to the presence of impurities. By matching the impurities' reflection with those of known phases, the sample contained a small amount of LaTa₃O₉ observed at 11°, 23°, 25°, and 57° and unreacted ZrO₂ at 30°, with 2.82% total weight fraction of LaTa₃O₉ at 72 hours heating duration. However, the intensity of LaTa₃O₉ and ZrO₂ reflections decreased gradually in time. The difficulty to decompose LaTa₃O₉ even when the sample was reheated longer is due to its high thermal stability, where the literature reported that LaTa₃O₉ melts congruently at 1850 ± 20 °C [6]. The low reactivity level of ZrO2 towards Ta2O5 and La2O3 raw materials contributed to the formation of LaTa₃O₉, since

 $LaTa_3O_9$ formation temperature was also at 1500 °C. Figure 2 shows the XRD profile of $LaZrTa_3O_{11}$ at different firing hours.

Electrical properties

LaZrTa₃O₁₁ pellets were characterised by IS using data collected from room temperature to high temperature in air. The pellet density calculated from the pellet mass and dimension was $\sim 91\%$ of the value expected for a fully dense pellet that was calculated from the unit cell dimensions and contents. The data were analysed as a function of frequency at fixed temperatures. Permittivity, ε at room temperature was low, \sim 19, of which from room temperature to 400 °C, the capacitance at high frequency plateau was ~ 1.7 pF/cm (Figure 3(a)), and within these temperatures, the sample was highly insulated, $R >> 10^9 \Omega$. Indeed, the conductivity, Y' data were too small to measure since the values were outside the machine limit. At a higher temperature range of 500 to 800 °C (Figure 3(b)), the data exhibited dispersion at a low frequency. The magnitude of C' increased from 10⁻¹¹ to 10⁻¹⁰ F/cm with decreasing frequency, suggesting that the response originated from either i) an interfacial or grain boundary capacitance, ii) the impurity phase, LaTa₃O₉, or iii) a bulk of CPE. The onset of dispersion to give a low capacitance plateau should be associated with any bulk response, which is observable at a higher frequency.

The admittance spectra, Y' of LaZrTa₃O₁₁ can only be measured above 600 °C, which showed a temperaturedependent behaviour in which Y' showed a power law response (Figure 4(a)). In the temperature range of 600 to 700 °C, the data set did not show a frequencyindependent admittance plateau at lower frequencies, however, at temperatures ≤ 700 °C, Y' decreased with decreasing frequency and tended to become independent of frequencies below a certain value. With increasing temperatures, there was evidence of lower frequency of direct current (DC) plateau that changed to a power law at higher frequencies. At 800 °C, a crossover between low-frequency dc plateau and high-frequency power law was clearly visible. Such behaviour is observed in many materials and is based on Jonscher's universal power law relation [8]:

$$\sigma_{\omega} = \sigma_o + A\omega^n \tag{1}$$

where, σ_o corresponds to bulk conductivity, σ_{dc} , σ_{ω} is the ac conductivity, A is a constant, ω is the angular frequency, and n is the power law exponent, where 0 < n < 1. The σ_{dc} value for LaZrTa₃O₁₁ was estimated and the Arrhenius law with the activation energy $\sim 1.1(2)$ eV was followed, as shown in Figure 4(b).

All the temperature data of C' against log f spectrum showed a similar trend of capacitance frequency-independent at a high frequency. The low conductivity of $6 \times 10^{-7} \ \Omega^{-1} \ \text{cm}^{-1}$ at $800^{\circ} \ \text{C}$ and the increasing capacitance from $10^{-12} \ \text{Fcm}^{-1}$ at room temperature to $10^{-11} \ \text{Fcm}^{-1}$ at $800^{\circ} \ \text{C}$ were due to the nonideality of the bulk response that can be represented by a CPE element. At a low temperature, the electrons were localised and possessed relatively very small thermal vibration and as the temperature increased to $700 \ ^{\circ} \ \text{C}$, these charges were capable of traversing the sample and therefore gave rise to direct current conduction. At higher temperatures, hopping conduction was easier since ions have a greater thermal energy and vibrate more vigorously, and also, defect concentrations are higher. The activation energy,

 E_a of the total conduction process was high, with the value of 1.1(2) eV whereby usually, a high activation energy is required for the occurrence of a thermally hopping type electronic mechanism.

Equivalent circuit analysis

In order to recognize which parameters contributed to the data shown in Figure 3 and Figure 4, it was essential to find an equivalent circuit that accurately represented the electrical response of LaZrTa₃O₁₁. The impedance data were modelled by using fitting programme, ZView Equivalent Circuit 2.9 Software. Appropriate frequency range data was selected, as some data may be seen unreliable due to instrument's limit at low frequencies and resonance effect for data above 1 MHz. The model started with a low temperature data which is usually related to bulk response in which some of the bulk parameters may be fixed to enable the modelling of higher temperature data which increasingly featured lower frequency phenomena, such as grain boundary. It is evident from Figure 3(b) and Figure 4(a) that LaZrTa₃O₁₁ ceramic sample showed a non-ideal Debye response, where it was usually described by adding a CPE to the parallel RC circuit element. Even though the specific meaning of CPE behaviour was not known, it was often used to describe the electrical behaviour of ionically conducting materials. CPE can be described by the relationship as follows:

$$Y^* = a(j\omega)^n = a\cos\left(n\frac{\pi}{2}\right) + j \ a \sin\left(n\frac{\pi}{2}\right)$$
$$= A\omega^n + jB\omega^n \tag{2}$$

where, $j = \sqrt{-1}$, A and B are interrelated by the admittance complex relationship, where $A = a \cos n(\pi/2)$, unit: Scm⁻¹rad⁻⁽ⁿ⁾, and $B = a \sin n(\pi/2)$, unit: Fcm⁻¹rad⁻⁽ⁿ⁻¹⁾. The value of the power law parameter, n was between 0 and 1 of which the capacitive or resistive behaviour of a material depended on the n value.

A summary of equivalent circuits used to fit data at different temperatures is shown in Figure 5. The impedance data collected from room temperature to 400° C can be represented by a simple, ideal, temperature-independent capacitor of magnitude ~ 1.7 pF/cm. At these temperature ranges, the Y' data cannot

be measured at any frequency, which indicated that the resistance, R was simply too large to measure. At temperatures ≥ 500 °C, the capacitance data showed a power law dependence on frequency, that the inclusion of a CPE may be required to fit the data. Therefore, a parallel combination of capacitor, C and CPE was used to fit the dispersions for the temperature range of 500 to 650 °C (Figure 5(b)). As the temperature reached \geq 650 °C, the Y' data showed frequency-dependent values at high frequencies, corresponding to AC conduction as well as the C' data showed a power law response at low frequencies of slope (n-1), which levelled off to a frequency-independent value at high frequencies. Therefore, for temperatures in the range of 675 to 800 °C, the dispersions may be fitted by using a parallel combination of RC circuit and CPE, as shown in Figure 5(c). The obtained values of the circuit parameters C, R, A, and n from the fits are summarized in Table 1. The R components of LaZrTa₃O₁₁ can only be measured at 675 °C and above. Its magnitude decreased with increasing temperature and magnitude of $A\omega^n$, and thus this represented that the frequency-dependent conductive component of the Y' data gradually increased in temperature. The magnitudes of bulk capacitance, C were fixed at high temperatures so as to enable the high temperature data to be fitted without unreasonable value of C, A, and n parameters.

It was possible to model the data accurately in terms of equivalent circuits by using the circuit that was frequently used to model the electrical properties of ionically conducting materials, which had a parallel combination of resistor, capacitor, and CPE. An associated capacitance of $1.663 \times 10^{-12} \, \mathrm{Fcm^{-1}}$ obtained at $651^{\circ}\mathrm{C}$ corresponded to C_b of the material. The CPE parameters, n and A showed changes in temperature. The n value showed intermediate low values from $n \sim 0.4$ to 0.27, which corresponded to intermediate behaviour between a frequency-dependent capacitor and resistor. The AC conductivity parameter, A showed an

increase in temperature, which indicated a thermal activation. Since most of the data showed no measurable DC conductivity, the conductivity was just limited to localized AC conductivity represented by parameter A, which was attributed to small atomic/electronic vibrations. These vibrations may be associated with the polarizable nature of the crystal structure from either Asite cation La, B-site cations Zr or Ta, or some oxygen. Like other insulators, these atomic displacements occurred only at high temperatures, with the activation energy of 1.1(2) eV. The resistivity, R was too large to be measured below the temperature of 675 °C of which the values fell from 9.8×10^7 to $2.3 \times 10^6 \,\Omega$ cm as the temperature increased. This could be associated with the increase in thermally activated drift mobility of electronic charge carriers by a hopping conduction mechanism. The circuit that is deduced in Figure 5(c) may be regarded as an extension of the ideal dielectric relaxation circuit in which the introduction of CPE added frequency-dependent elements to the single-value components, R and C. By excluding the CPE element, the circuit was often used to represent dielectric relaxation processes within an insulating system, which were composed of ideal, frequency-independent circuit elements.

The ε value of a compound was closely related to the stability of material's crystal structure, and thus oxides crystallized in the hexagonal structure should exhibit higher ε values than the oxides crystallized in the cubic and monoclinic ones. In this study, the capacitance value, $C' \sim 1.663 \times 10^{-12} \, \mathrm{Fcm^{-1}}$, ($\varepsilon \sim 19$) exhibited by LaZrTa₃O₁₁ was what the researchers expected from lanthanide oxides-based materials in which the value was comparable to the literature which reported that early rare-earth materials possessed intermediate dielectric constants ($\varepsilon \sim 12\text{-}20$) with large band gaps of $\sim 5.4 \, \mathrm{eV}$ [9].

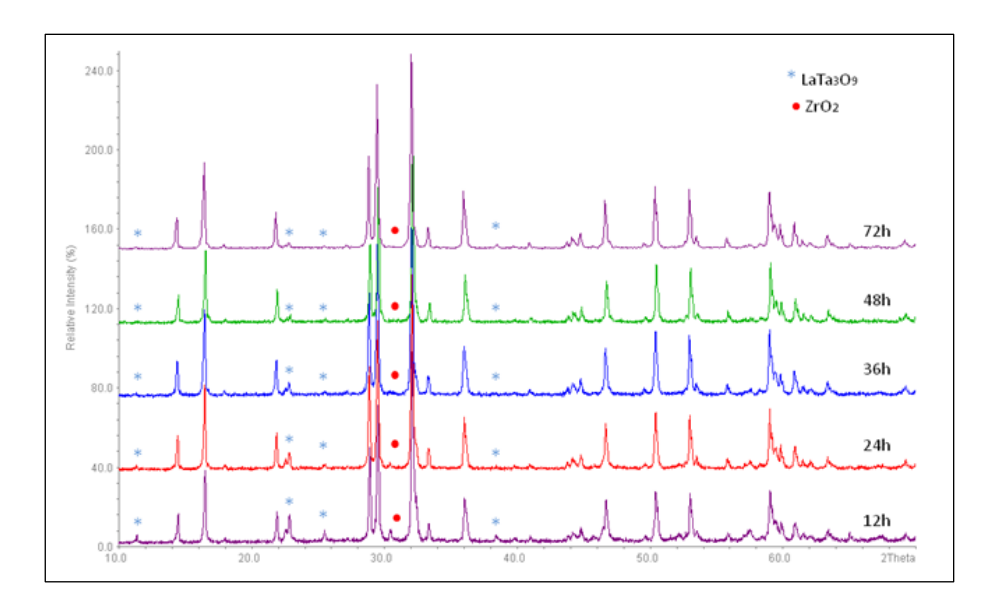


Figure 2. XRD profiles for LaZrTa $_3$ O $_{11}$ using La $_2$ O $_3$, Ta $_2$ O $_5$ and ZrO $_2$ as starting reagents. The sample was heated from 12 to 72 hours at 1500 °C

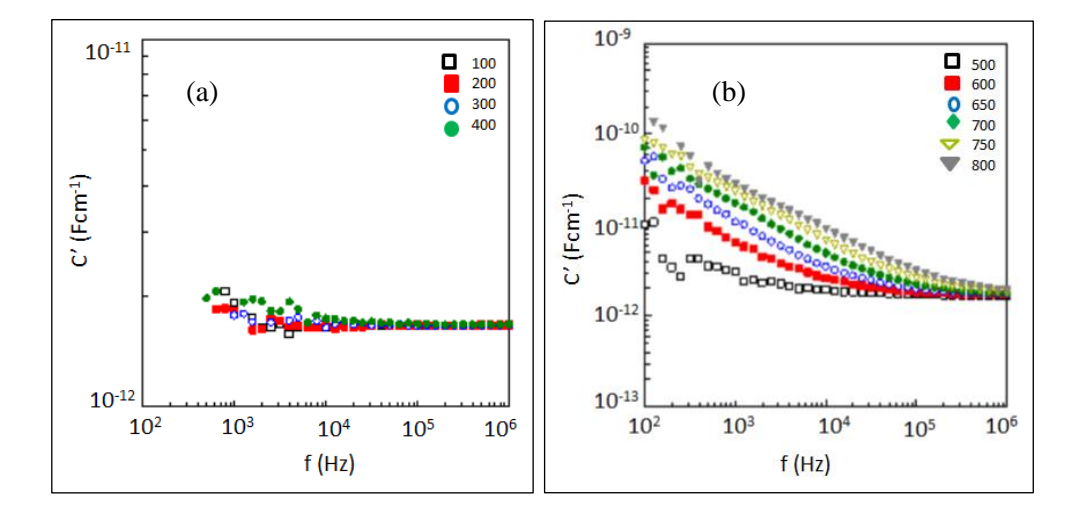


Figure 3. Capacitance, C' versus frequency for temperatures (a) 100 to 400 °C (b) 500 to 800° C

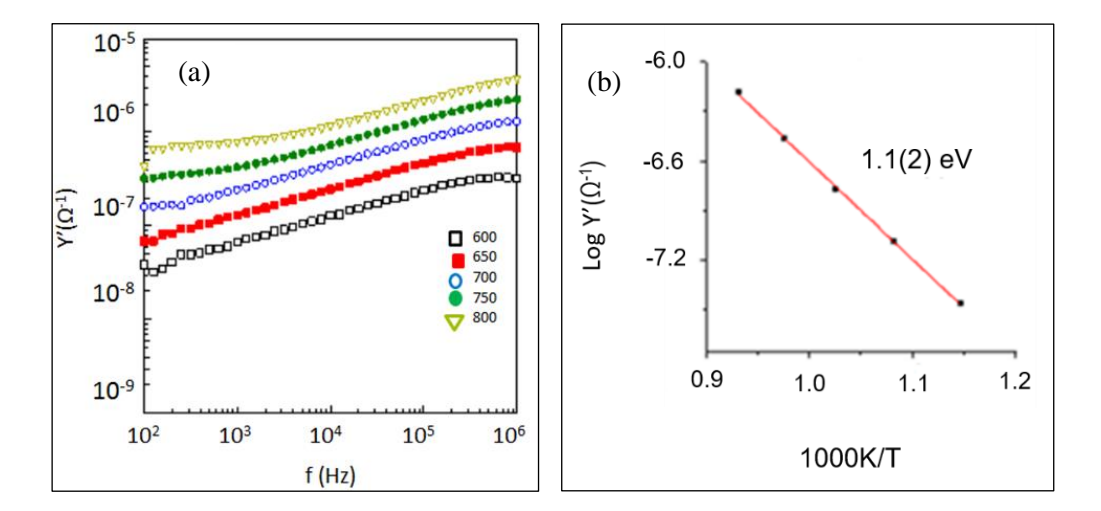


Figure 4. (a) Admittance, Y' versus frequency for 500 to 800 °C (b) Arrhenius plot of the total admittance, Y'

Temperature (° C)	Circuit			
Room temperature – 400	(a) C1			
500 – 650	(b) C1 CPE1			
675 – 800	(c) C1 R1 CPE1 >>			

Figure 5. Equivalent circuits used at different temperatures, (a) simple capacitor from room temperature to 400 $^{\circ}$ C, (b) parallel combination of a capacitor and a CPE at temperature range of 500 to 650 $^{\circ}$ C, and (c) non-ideal Debye circuit for temperatures from 675 to 800 $^{\circ}$ C

Table	1. Fitting	parameters data	of C , A , n , and R from	om room t	emperature to 80	0°C
	T (0C)	C (E -1)	4 (C -1 I-n)		D (O)	

T (°C)	C (Fcm ⁻¹)	A (Scm ⁻¹ rad ⁻ⁿ)	n	R (Qcm)
23	$1.68(1) \times 10^{-12}$	-	-	-
100	$1.67(1) \times 10^{-12}$	-	-	-
200	$1.672(9) \times 10^{-12}$	-	-	-
300	$1.70(1) \times 10^{-12}$	-	-	-
400	$1.66(2) \times 10^{-12}$	$1.0(4) \times 10^{-10}$	0.41(4)	-
500	$1.67(9) \times 10^{-12}$	$8.9(7) \times 10^{-10}$	0.323(8)	-
600	$1.673(5) \times 10^{-12}$	$6.5(1) \times 10^{-9}$	0.277(1)	-
625	$1.667(4) \times 10^{-12}$	$9.3(1) \times 10^{-9}$	0.277(1)	-
651	$1.663(4) \times 10^{-12}$	$1.27(2) \times 10^{-8}$	0.276(1)	-
676	1.663×10^{-12}	$1.5(2) \times 10^{-8}$	0.28(1)	$9.8(8) \times 10^7$
702	1.663×10^{-12}	$1.6(1) \times 10^{-8}$	0.294(5)	$2.2(3) \times 10^7$
726	1.663×10^{-12}	$1.6(1) \times 10^{-8}$	0.311(5)	$9.8(7) \times 10^6$
751	1.663×10^{-12}	$1.7(1) \times 10^{-8}$	0.321(5)	$5.5(3) \times 10^6$
775	1.663×10^{-12}	$2.0(2) \times 10^{-8}$	0.324(7)	$3.5(2)\times10^6$
800	1.663×10^{-12}	2.3×10^{-8}	0.32(1)	$2.3(2) \times 10^6$

Conclusion

LaZrTa₃O₁₁ was prepared by using the conventional solid-state route and studied by using XRD and IS electrical measurements. It had a hexagonal space group, $P6_322$ of a larger unit cell, a ≈ 6.28 and $c \approx 12.45$ Å as compared to the literature. The structure consisted of layers of edge-sharing pentagonal Ta-O bipyramids, which alternated with layers of edge-sharing octahedral. The IS response showed that LaZrTa₃O₁₁ exhibited a typical insulating behaviour, i.e., low permittivity, $\varepsilon \sim$ 19 with a large value of activation energy, $E_a \sim 1.1(2)$ eV; dispersion of capacitance at low frequencies and frequency-independent capacitance at high frequencies were also observed. LaZrTa₃O₁₁ sample showed a highly resistive material of R >> $10^9 \Omega$ at temperatures below 500 °C. As the temperatures went higher than 675 °C, frequency-dependence of AC conductivities at high frequency was observed; DC conductivities were observed as the temperature increased further. The electrical properties may be accurately modelled by using the non-ideal Debye response circuit, which consisted of a parallel combination of resistor, capacitor,

and CPE elements. The introduction of CPE into the equivalent circuit may be an indication of nonideality in the bulk conduction mechanism for LaZrTa₃O₁₁, which was electrically homogeneous in terms of its electrical microstructure. The insulating behaviour as well as the interesting structure of LaZrTa₃O₁₁ were noted in the literature [1, 2], and thus this type of material could potentially be used for dielectric applications.

Acknowledgement

The researchers would like to thank Universiti Pertahanan Nasional Malaysia (UPNM) and the Ministry of Higher Education Malaysia (MOHE) for their financial support through the Fundamental Research Grant Scheme (FRGS/1/2017/STG07/UPNM/02/2) as well as the Engineering and Physical Sciences Research Council (EPSRC) for funding this research.

References

- Masó, N., Woodward, D. I., Thomas, P. A., Várez, A. and West, A. R. (2011). Structural characterisation of ferroelectric Ag₂Nb₄O₁₁ and dielectric Ag₂Ta₄O₁₁. Journal of Materials Chemistry, 21: 2715-2722.
- 2. Grins, J. and Nygren, M. (1992). Structure of LaZrTa₃O₁₁, a CaTa₄O₁₁ isotype. *Materials Research Bulletin*, 27: 141-145.
- 3. Masó, N., Woodward, D. I., Thomas, P. A., Várez, A. and West, A. R. (2011). Polymorphism, structural characterisation and electrical properties of Na₂Nb₄O₁₁. *Journal of Materials Chemistry*, 21: 12096-12102.
- 4. Fadhlina Che Ros, Mclaren, N. R., Masó, N. and West, A. R. (2018). Synthesis, structure and dielectric properties of a new family of phases, ABC₃O₁₁: A = La, Pr, Nd, Sm, Gd; B = Zr, Hf; C =

- Ta, Nb. *Journal of Australian Ceramic Society*, 54: 1-10.
- 5. Jahnberg, L. (1970). Crystal structures of Na₂Nb₄O₁₁ and CaTa₄O₁₁. *Journal of Solid State Chemistry*, 1: 454-462.
- Zheng, C. and West, A. R. (1991). Compound and solid-solution formation, phase equilibria and electrical properties in the ceramic system ZrO₂-La₂O₃-Ta₂O₅. *Journal of Materials Chemistry*, 1(2): 163-167.
- 7. Moulson, A. J. and Herbert, J. M. (2008) Electroceramics. John Wiley & Sons: pp. 285.
- 8. Joncher, A. K. (1983). Dielectric relaxation in solids. chelsea dielectric press. London: pp. 209.
- 9. Scarel, G., Svane, A. and Fanciulli, M., (2007). Scientific and technological issue related to rare–earth oxides: An introduction. *Journal of Applied Physics*, 106: 1-14.